Colorimetric Response of Dithizone Product and Hexadecyl Trimethyl Ammonium Bromide Modified Gold Nanoparticle Dispersion to 10 Types of Heavy Metal Ions: Understanding the Involve...

ARTICLE *in* LANGMUIR · MAY 2013

Impact Factor: 4.46 · DOI: 10.1021/la400909b · Source: PubMed

6 AUTHORS, INCLUDING:

An Gong
Center of Advanced European Studies and Res...
14 PUBLICATIONS **64** CITATIONS
SEE PROFILE

Zheyu Shen
Chinese Academy of Sciences
32 PUBLICATIONS **577** CITATIONS
SEE PROFILE

Liang Chen
National University of Defense Technology
110 PUBLICATIONS **1,382** CITATIONS
SEE PROFILE

Aiguo Wu
Chinese Academy of Sciences
112 PUBLICATIONS **1,722** CITATIONS
SEE PROFILE

Langmuir

Article

pubs.acs.org/Langmuir

Colorimetric Response of Dithizone Product and Hexadecyl Trimethyl Ammonium Bromide Modified Gold Nanoparticle Dispersion to 10 Types of Heavy Metal Ions: Understanding the Involved Molecules from Experiment to Simulation

Yumin Leng, Yonglong, Li, An Gong, Zheyu Shen, Liang Chen,* and Aiguo Wu*

Key Laboratory of Magnetic Materials and Devices, and Division of Functional Materials and Nanodevices, and New Energy Institute, Ningbo Institute of Materials Technology & Engineering (NIMTE), Chinese Academy of Sciences (CAS), Ningbo 315201, China

Supporting Information

ABSTRACT: A new kind of analytical reagent, hexadecyl trimethyl ammonium bromide (CTAB), and dithizone product-modified gold nanoparticle dispersion, is developed for colorimetric response to 10 types of heavy metal ions (M^{n+}), including Cr(VI), Cr^{3+}, Mn^{2+}, Co^{2+}, Ni^{2+}, Cu^{2+}, Zn^{2+}, Cd^{2+}, Hg^{2+}, and Pb^{2+}. The color change of the modified gold nanoparticle dispersion is instantaneous and distinct for Mn^{2+}, Co^{2+}, Ni^{2+}, Cu^{2+}, Zn^{2+}, Cd^{2+}, Hg^{2+}, and Pb^{2+}. The color change results from the multiple reasons, such as electronic transitions, cation−π interactions, formation of coordination bonds, and M^{n+}-induced aggregation of gold nanoparticles (AuNPs). The different combining capacity of heavy metal ions to modifiers results in the different broadening and red-shifting of the plasmon peak of modified AuNPs. In addition, Cr(VI), Cu^{2+}, Co^{2+}, Ni^{2+}, and Mn^{2+} cause the new UV−vis absorption peaks in the region of 360−460 nm. The interactions between the modifiers and AuNPs, and between the modifiers and M^{n+}, are investigated by using Fourier transform infrared spectroscopy and X-ray photoelectron spectroscopy. The results confirm that AuNPs are modified by CTAB and dithizone products through electrostatic interactions and Au−S bonds, respectively, and the M^{n+}−N bonds form between M^{n+} and dithizone products. Furthermore, the experimental and density functional theory calculated IR spectra prove that dithizone reacts with NaOH to produce $C_6H_5O^-$ and $[SCH_2N_4]^{2-}$. The validation of this method is carried out by analysis of heavy metal ions in tap water.

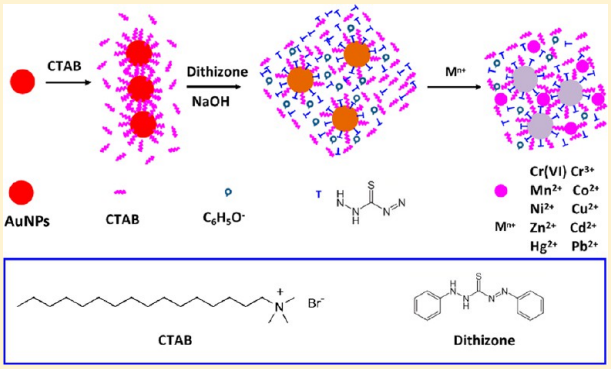

INTRODUCTION

Synthesis of analytical reagents containing functionalized nanoparticles for sensing biological and chemical species has attracted increasing attention.[1−9] Detection of targets by reagents has been performed with the use of UV−vis spectroscopy, the fluorescence method, electrochemical detection, and colorimetric assays.[10−17] The AuNPs-based colorimetric reagents provide simplicity and excellent detection capability for a variety of targets, including protein, DNA, small molecules, and metal ions.[1−3,5,6,8−13,17] Among these targeted species, heavy metal ions have been a major concern throughout the world for several decades[1−3,6,9,12−14,17] because exposure to high levels of Cr(VI), Mn^{2+}, Co^{2+}, Ni^{2+}, Cu^{2+}, Zn^{2+}, Cd^{2+}, Hg^{2+}, and Pb^{2+} causes quite serious long-term damage to human beings and animals. For example, the toxicological effects of Co^{2+} on human beings may lead to terrible diseases, such as anemia and cardiomyopathy.[18,19] Cu^{2+} and Ni^{2+} are toxic at high concentrations and can cause cancer, liver, and kidney damage.[20,21] In recent years, the analytical reagents of functionalized AuNPs with high selectivity and sensitivity were developed for colorimetric detection of heavy metal ions, such as Pb^{2+} and Hg^{2+},[2,9,17] which bring serious adverse effects, even at relatively low concentrations.[22,23] Besides, simultaneous colorimetric sensing of several heavy metal ions with the use of functionalized AuNPs reagents was also reported.[1,3,24−27] For example, the functionalized AuNPs dispersions were used for simultaneous colorimetric response to Pb^{2+}, Co^{2+} and Hg^{2+},[3] Hg^{2+} and Pb^{2+},[24−26] or Pb^{2+}, Cu^{2+}, and Hg^{2+}.[27] But only two or three heavy metal ions could be simultaneously detected by the reported reagents. Here, we propose a novel reagent of AuNPs modified by hexadecyl trimethyl ammonium bromide (CTAB) and dithizone products for simultaneous colorimetric response to 10 types of heavy metal ions, including Cr(VI), Cr^{3+}, Mn^{2+}, Co^{2+}, Ni^{2+}, Cu^{2+}, Zn^{2+}, Cd^{2+}, Hg^{2+}, and Pb^{2+}. Moreover, we extend our effort to investigate the molecular structures, using both the experimental means and density functional theory (DFT) calculations.

Received: December 6, 2012
Revised: May 17, 2013
Published: May 31, 2013

Experimentally, Fourier-transform-infrared (FT-IR) spectroscopy has become an accepted tool for the characterization of IR spectra associated with molecular vibrations.[13,28] Theoretically, DFT has been proven to be a powerful tool for determining the structures, vibrational frequencies, and interaction mechanisms of molecules.[28−30] Therefore, we use DFT calculations to determine the involved molecular structures in the experiment and simulate their vibrational frequencies compared with the experimental FT-IR results. The calculated IR spectra are in good agreement with the corresponding experimental ones, showing that dithizone reacts with NaOH to create $C_6H_5O^-$ and $[SCH_2N_4]^{2-}$. The FT-IR and X-ray photoelectron spectroscopy (XPS) characterizations verify the attachment of CTAB headgroups $[-(CH_3)_3NBr]$ on AuNPs. The FT-IR and XPS results also prove that AuNPs are modified by $[SCH_2N_4]^{2-}$ through Au−S bonds and heavy metal ions (M^{n+}) are recognized by $[SCH_2N_4]^{2-}$ through M^{n+}−N bonds. In addition, the developed reagent is also validated by analysis of the spiked heavy metal ions in tap water. Interestingly, the colorimetric response and optical response [surface plasmon resonance (SPR) peak] are distinct and reproducible for a particular metal ion. The color change results from multiple reasons, such as electronic transitions, cation−π interactions, formation of coordination bonds, and M^{n+}-induced aggregation of gold nanoparticles (AuNPs).

EXPERIMENTAL SECTION

Materials and Instrumentation. Chloroauric acid tetrahydrate ($HAuCl_4{\cdot}4H_2O$), hexadecyl trimethyl ammonium bromide (CTAB), sodium borohydride ($NaBH_4$), dithizone, NaCl, KCl, $CaCl_2$, $SrCl_2{\cdot}6H_2O$, $AlCl_3$, $FeCl_3$, $K_2Cr_2O_7$, $CrCl_3{\cdot}6H_2O$, $MnCl_2{\cdot}4H_2O$, $CoCl_2{\cdot}6H_2O$, $NiCl_2{\cdot}6H_2O$, $ZnCl_2$, $CdCl_2{\cdot}2.5H_2O$, $HgSO_4$, and $Pb(NO_3)_2$ were obtained from Sinopharm Chemical Reagent Company, Ltd. (Beijing, China). LiCl, $BaCl_2{\cdot}2H_2O$, $MgCl_2{\cdot}6H_2O$, $FeCl_2{\cdot}4H_2O$, and $CuSO_4{\cdot}5H_2O$ were obtained from Aladdin-regent Company Ltd. (Shanghai, China). All chemicals were used as received, without further purification. All glassware were washed with aqua regia [HCl/HNO_3 = 3:1 (v/v), a strong corrosive], and then cleaned with Milli-Q water.

FT-IR spectroscopy was performed using a Nicolet 6700 spectrometer. Transmission electron microscopy (TEM) was performed on a Tencai F20 instrument and operated at 200 kV. UV−vis absorption spectra were recorded using a Lambda 950 UV−vis spectrophotometer from Perkin-Elmer. XPS was performed using an AXIS Ultra DLD instrument with Mg Kα radiation as the X-ray source.

Synthesis of Analytical Reagent and Sensing Metal Ions. In accordance with Murphy's method,[31] the AuNPs were prepared by reducing $HAuCl_4$ with $NaBH_4$ in the presence of CTAB. In brief, 5 mL of $HAuCl_4$ solution (5×10^{-3} M) was added to 95 mL of Milli-Q water, under vigorous stirring. Three milliliters of CTAB solution (3.5×10^{-3} M) was then injected into the mixture. After that, 1.5 mL of freshly prepared $NaBH_4$ solution (0.1 M) was injected slowly. The reaction was kept for 30 min, during the time the color changed from pink to deep red. The CTAB capped AuNPs (CTAB AuNPs) dispersion was stored at 4 °C for more than 24 h. Finally, 0.5 mL of dithizone solution (5.5×10^{-3} M, dissolved in 0.2 M NaOH solution) was slowly added into 22 mL of the as-synthesized CTAB AuNPs. The developed reagent was stored at 4 °C until use.

The colorimetric sensing of heavy metal ions using the developed reagent was performed by mixing 80 μM heavy metal ions with the developed reagent at a volume ratio of 1:3.

Structure and Frequency Calculations. The geometry optimizations on the structures of dithizone before and after dissolved in NaOH solution were performed by means of DFT methods using Gaussian03. The vibrational frequencies of dithizone and dithizone products were calculated at the B3LYP/6-31G* level.[13,29,32,33] The vibrational frequencies were scaled with the factors of 0.92, 0.98, and 1.05, according to refs 34, 35.

RESULTS AND DISCUSSION

Characterizations of the Developed Reagent. The UV−vis absorption spectra of CTAB AuNPs dispersion, dithizone solution, and the developed reagent (the CTAB AuNPs were modified by dithizone) are shown in Figure 1.

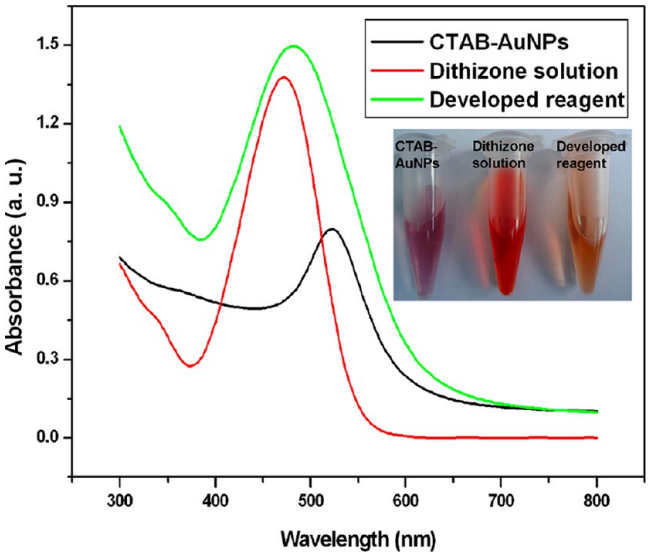

Figure 1. Comparison of UV−vis absorption spectra of CTAB AuNPs dispersion, dithizone solution, and the developed reagent of CTAB AuNPs modified by dithizone solution. The inset: colors of CTAB AuNPs dispersion, dithizone solution, and the developed reagent.

Their corresponding colors can be seen in the inset of Figure 1. The wavelengths of maximum absorption for CTAB AuNPs and the developed reagent are determined to be 524 and 480 nm, respectively. The absorption maxima for $n \rightarrow \sigma^*$ transition for dithizone solution is found as 472 nm. The UV−vis absorption spectrum of developed reagent is contributed by both CTAB AuNPs and dithizone solutions.

As the freshly prepared CTAB AuNPs dispersion was stored at 4 °C for more than 24 h, the chainlike CTAB AuNPs were formed (see Figure 2A). The chainlike CTAB AuNPs were dispersed by the modifier of dithizone (see Figure 2B), and the average size of modified AuNPs was measured to be ~15 nm.

In order to investigate the structure changes of dithizone after dissolution in NaOH solution, we applied both computational and experimental techniques to characterize the relative molecular structures and vibrational frequencies. When dithizone is dissolved in NaOH solution, the chemical reaction may happen as shown in Figure 3A. Dithizone may react with NaOH to produce phenol (C_6H_5OH) and $SCH_2N_4Na_2$, and the product of phenol (C_6H_5OH) is easily neutralized by NaOH forming sodium phenate (C_6H_5ONa). Computationally, for conformational explorations, the structures of dithizone before and after dissolution in the NaOH solution (see Figure 3B) were obtained by extensive DFT calculations. Experimentally, dithizone was dissolved in 0.2 M NaOH solution and then vacuum freeze-dried. The powders of dithizone and dithizone products were characterized by FT-IR spectroscopy, respectively. In order to ascertain the accuracy of calculated configurations, the vibrational frequencies of the optimized structures of dithizone and dithizone products ($C_6H_5O^-$ and

dx.doi.org/10.1021/la400909b | Langmuir 2013, 29, 7591−7599

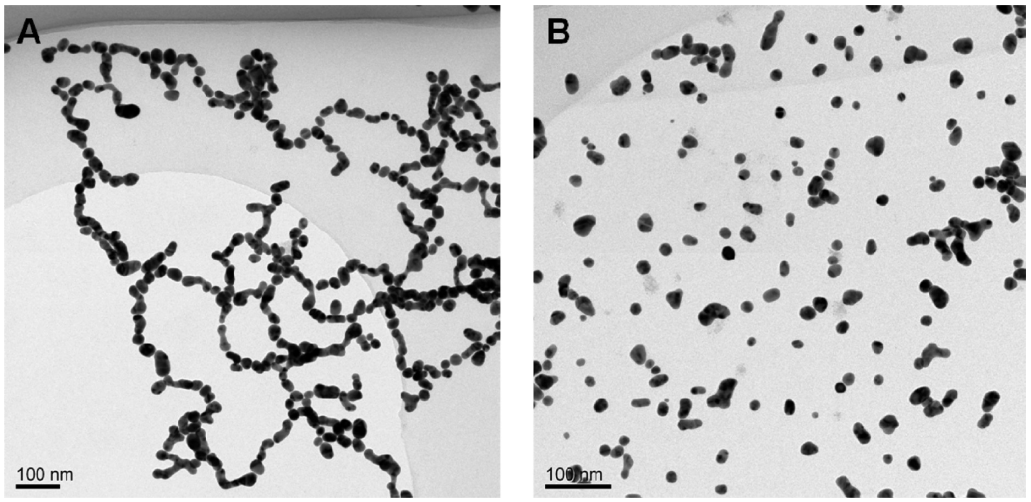

Figure 2. TEM images of (A) CTAB AuNPs and (B) CTAB AuNPs modified by dithizone.

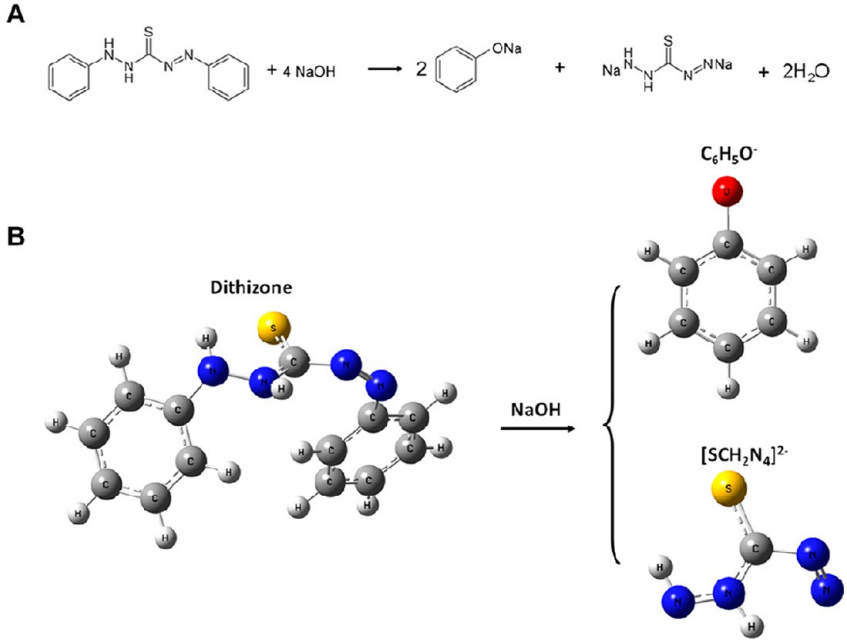

Figure 3. (A) Chemical reaction for dithizone reacted with NaOH. (B) Simulated structures of dithizone before and after dissolution in NaOH solution.

$[SCH_2N_4]^{2-}$) were calculated at the B3LYP/6-31G* level and compared with the experimental FT-IR spectra (see Figure 4). Most characteristic peaks of the calculated IR spectra of dithizone and dithizone products (the coupling frequencies of $C_6H_5O^-$ and $[SCH_2N_4]^{2-}$) are in agreement with that presented in the experiments, respectively (see Figure 4). The experimental and simulated IR peaks of dithizone at ~3487, 3095, 1600, 1442, 1311, 1143, and 677 cm^{-1} correspond to the N−H, C−H, C−C, N═N, N−C (the C of benzene ring), N−C (the C attached to S), and C═S stretching vibrations, respectively. For dithizone products, the consistent frequencies of the N−H, C−H, N−N, C−C, N═N, N−C, C−O, and C═S stretching vibrations appeared in the experimental and calculated IR spectra are ~3471, 3095, 1670, 1600, 1458, 1114, 863, and 697 cm^{-1}, respectively.

When the dithizone solution is saved for 3 and 7 days at 25 °C, its color becomes shallow gradually and its UV−vis absorption peak at 472 nm disappears (see Figure S1 of the Supporting Information). The reaction products of C_6H_5ONa and $SCH_2N_4Na_2$ in alkaline solution might be unstable and combine with O_2 from the atmosphere to create some other small molecules, the UV−vis absorption peaks of which appeared in the region of 300−400 nm (see Figure S1 of the Supporting Information).

To study the interactons between the modifiers of CTAB/dithizone products and AuNPs, we used FT-IR spectroscopy and XPS to measure the relative IR spectra and binding energies, respectively. The IR spectra of dithizone products, CTAB AuNPs, and the develeped reagent are shown in Figure 5. The Au···N and Au···Br stretching vibrations at 175 cm^{-1} and 188 cm^{-1} (See Figure 5A), as well as the previously reported values,[36,37] indicate that the CTAB molecules adsorb on AuNPs with their headgroups $[-(CH_3)_3NBr]$. As reported in the literature, CTAB molecules adsorb on the surface of AuNPs in the form of a bilayer to form a hydrophilic out layer so the CTAB AuNPs can be well-dispersed in an aqueous

dx.doi.org/10.1021/la400909b | Langmuir 2013, 29, 7591−7599

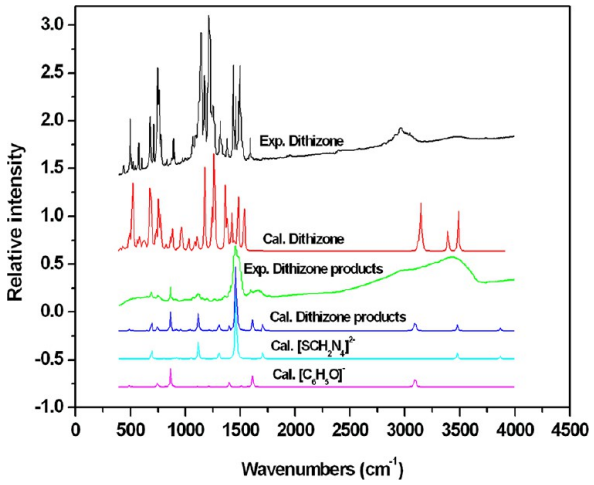

Figure 4. Experimental and calculated IR spectra for dithizone before and after dissolution in NaOH solution. The calculated IR spectra for dithizone products is the coupling frequencies of the simulated structures of $C_6H_5O^-$ and $[SCH_2N_4]^{2-}$.

solution.[38−40] To further verify the interactions between CTAB molecules and AuNPs, we used XPS to characterize the binding energies of characteristic elements of CTAB (C, N, and Br) before and after its modification on AuNPs. As shown in Figure 6, there are XPS spectra peaks for C 1s, N 1s, and Br 3d. The binding energy (284.7 eV) of the C 1s component has no change before and after AuNPs capped by CTAB (see Figure 6, C1s). Relative to pure CTAB, the N 1s peak is blue shifted by 0.2 eV (see Figure 6, N1s) and the significant new peak appeares at 63.3 eV in the spectra of Br 3d (See Figure 6, Br3d) after binding to the surface of the AuNPs. The changes of N 1s and Br 3d peaks imply that the interactions between CTAB headgroups $[-(CH_3)_3NBr]$ and AuNPs induce CTAB molecules to absorb on the surface of AuNPs. The polar head $[-(CH_3)_3N^+]$ of CTAB is facing AuNPs surfaces by forming surface ion pairs with Br^- ions; the electrostatic interactions between $C_{16}H_{33}(CH_3)_3N^+$ and Br^- induce CTAB molecules to attach on AuNPs.[41,42] In the far-IR spectra of the developed reagent (see Figure 5A), the peak at 265 cm^{-1}, which is Au−S stretching as previously observed,[43] verifies the formation of Au−S bonds between AuNPs and $[SCH_2N_4]^{2-}$. In addition, except the combination of the vibrational modes of CTAB AuNPs and dithizone products which appeared in the IR spectra of the developed reagent, the new peak appeared at 3538 cm^{-1} can be attributed to the N···H stretch (see Figure 5B).[28,44] The experimental results demonstrate that AuNPs are modified by CTAB and $[SCH_2N_4]^{2-}$ through electrostatic interactions and Au−S bonds, respectively, and the hydrogen bonds (N···H) are formed among the modifiers.

Colorimetric Response of the Developed Reagent to Heavy Metal Ions. We first tested whether the developed reagent can be a colorimetric response to heavy metal ions. The assumption was that the binding of heavy metal ions by the modifiers of CTAB and $[SCH_2N_4]^{2-}$ would result in the aggregation of dispersed AuNPs via bridging of neighboring AuNPs (see Scheme 1) or by affecting the charge distribution between modifiers and heavy metal ions. Addition of 20 μM heavy metal ions such as Cr(VI), Cr^{3+}, Mn^{2+}, Co^{2+}, Ni^{2+}, Cu^{2+}, Zn^{2+}, Cd^{2+}, Hg^{2+}, and Pb^{2+} to the developed reagent result in a distinct color change (Figure 7A). The colorimetric response of the developed reagent in the presence of Co^{2+}, Ni^{2+}, Cu^{2+}, Zn^{2+}, Cd^{2+}, Hg^{2+}, Pb^{2+}, and Mn^{2+} is immediate (see the video of the Supporting Information), while Cr(VI) and Cr^{3+} take 1 h.

As the properties associated with AuNPs can generally be exhibited by UV−vis absorption spectroscopy,[1,3,5,12,13] herein, the UV−vis absorption spectra of the developed reagent and its mixtures with heavy metal ions are shown in Figure 7. The corresponding maximum absorption wavelength are shown in Table S1 of the Supporting Information. Addition of heavy metal ions to the developed reagent results in the broadening and different red shifting of the plasmon peak (See Figure 7, panels B and C), which is due to the different aggregation of AuNPs induced by heavy metal ions. The TEM images of AuNPs aggregated by heavy metal ions (i.e., Hg^{2+} and Co^{2+}) are shown in Figure S2 of the Supporting Information. Interestingly, Cr(VI), Cu^{2+}, Co^{2+}, Ni^{2+}, and Mn^{2+} also cause new absorption peaks, appearing in the region of 360−460 nm (see Figure 7C). The reason might be that the charges transfer from the modifiers of $[SCH_2N_4]^{2-}$ to Cr(VI)/Cu^{2+}/Co^{2+}/Ni^{2+}/Mn^{2+},[45−48] and the different excited states are then mixed in these heavy metal ions, resulting in a more complex UV−vis absorption. Although the developed reagent seems not selective

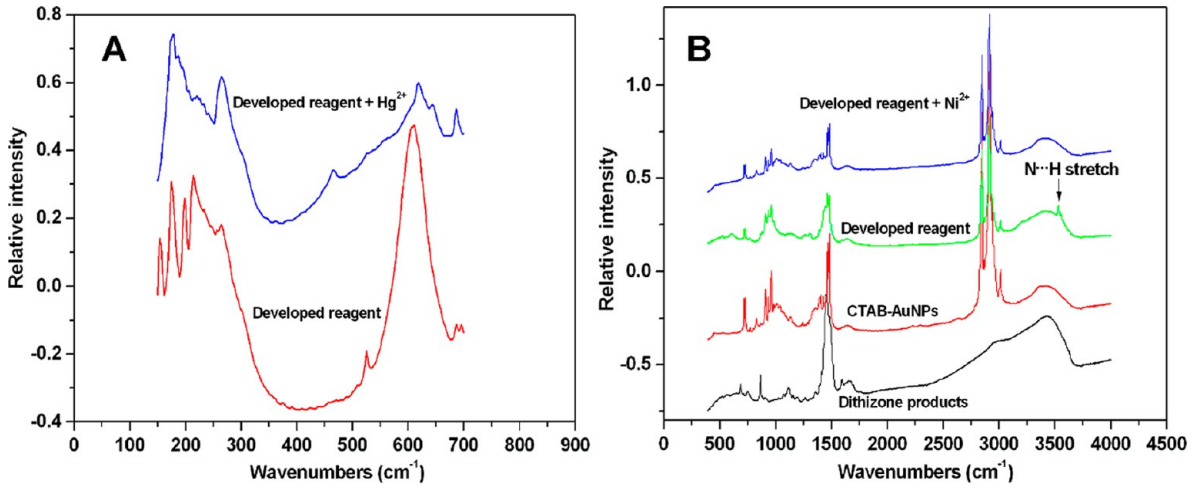

Figure 5. (A) Experimental far-IR spectra of the developed reagent and its mixture with Hg^{2+} in the region of 150−700 cm^{-1}. (B) Experimental IR spectra of the dithizone products, CTAB AuNPs, developed reagent, and developed reagent in the presence of Ni^{2+}, in the region of 500−4000 cm^{-1}.

dx.doi.org/10.1021/la400909b | Langmuir 2013, 29, 7591−7599

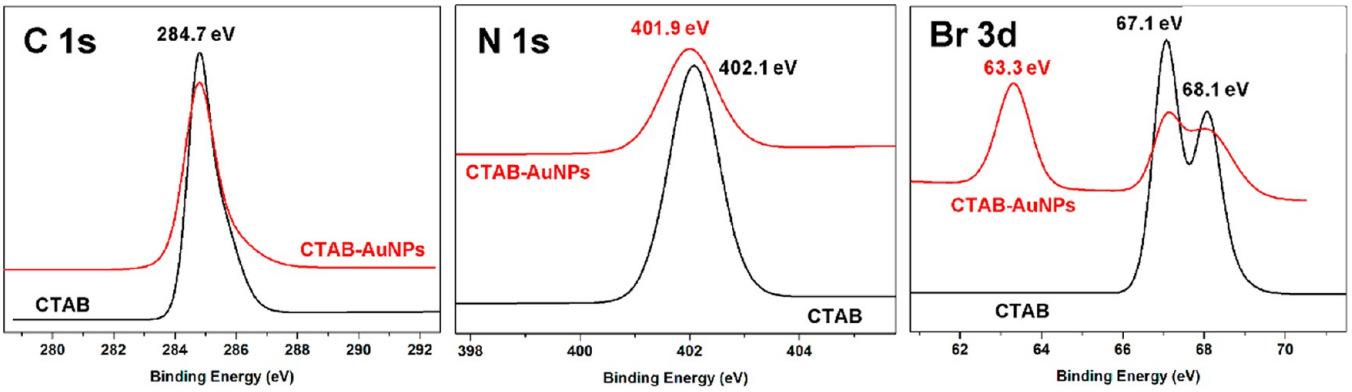

Figure 6. Comparison of the C 1s, N 1s, and Br 3d XPS spectra before and after AuNPs modified by CTAB.

Scheme 1. Schematic Illustration of the AuNPs Modified by CTAB and Dithizone Products and Their Aggregation in the Presence of Heavy Metal Ions

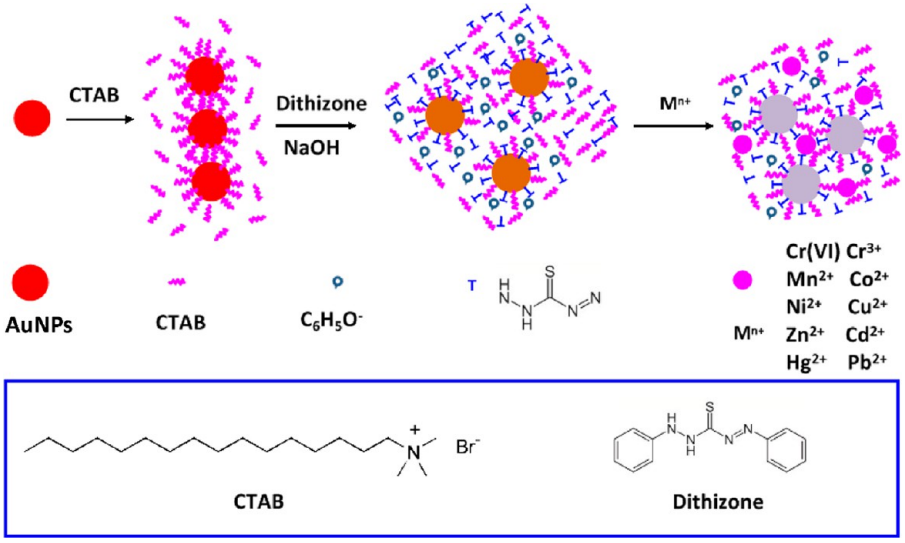

for a particular heavy metal ion, the optical response (color changes and SPR absorption peak) of the developed reagent is found to be characteristic for a given heavy metal ion.

To evaluate the sensitivity of our system, different concentrations (10^{-8} ~ 10^{-5} M) of heavy metal ions were tested (see Figure S3A of the Supporting Information). The colorimetric response limits for the tested heavy metal ions are up to 10^{-5} M. The developed reagent for Cu^{2+} sensing is sensitive, as the detection limit of 10^{-5} M is lower than the sanitary standard of drinking water (1.6×10^{-5} M).[49] Addition of different concentrations of Cu^{2+} ranging from 0 to 10^{-1} M to the developed reagent results in a distinct color change (see Figure S3B of the Supporting Information). Although the color changes of the developed reagent in the presence of 10^{-4} M Cu^{2+} and 2×10^{-5} M Mn^{2+} are similar, the corresponding UV–vis absorption spectra are very different (see Figure S4 of the Supporting Information).

Furthermore, we also investigated the colorimetric response of the developed reagent to other metal ions and whether the color changes of CTAB and dithizone solutions are induced by heavy metal ions. The developed reagent has no color change after being mixed with 20 μM Li^+, Na^+, K^+, Ca^{2+}, Ba^{2+}, Sr^{2+}, Al^{3+}, Mg^{2+}, Fe^{2+}, and Fe^{3+} (see Figure S5 of the Supporting Information). As shown in Figure S6, panel A, of the Supporting Information, there is no colorimetric response of the CTAB AuNPs solution in the presence of heavy metal ions (20 μM). However, after addition of the dithizone solution, only Co^{2+} results in a rapid color change (see Figure S6, panel B, of the Supporting Information). In addition, the mixture of CTAB and dithizone solution can be colorimetric response to five types of heavy metal ions (Co^{2+}, Cu^{2+}, Zn^{2+}, Hg^{2+}, and Pb^{2+}) (see Figure S6, panel C, of the Supporting Information). As reported in literature,[50] these heavy metal ions should acquire electrons to fill their valence orbits by forming bonds to the ligands of CTAB and dithizone products that act as electron donors. The colors result from electronic transitions between partially filled orbits (d–d transitions), which are split into lower energy and higher energy.[50] To further determine the reason for the color changes, we characterized the mixture of CTAB and dithizone solutions with heavy metal ions by UV–vis spectrometry (see Figure S7A of the Supporting Information). The absorption peaks of the complexes of CTAB and dithizone products with heavy metal ions appear in the region of 520–570 nm (see Figure S7, panel A, of the Supporting Information). The ratio ($A_{chelates}/A_{reagents}$) of the absorption peak intensity of the chelates over that of the mixture of CTAB and dithizone solution is used to express the molar ratio of chelates and free reagents (CTAB and dithizone products) (see Figure S7, panel B, of the Supporting Information). The corresponding ratios are in the following

dx.doi.org/10.1021/la400909b | Langmuir 2013, 29, 7591–7599

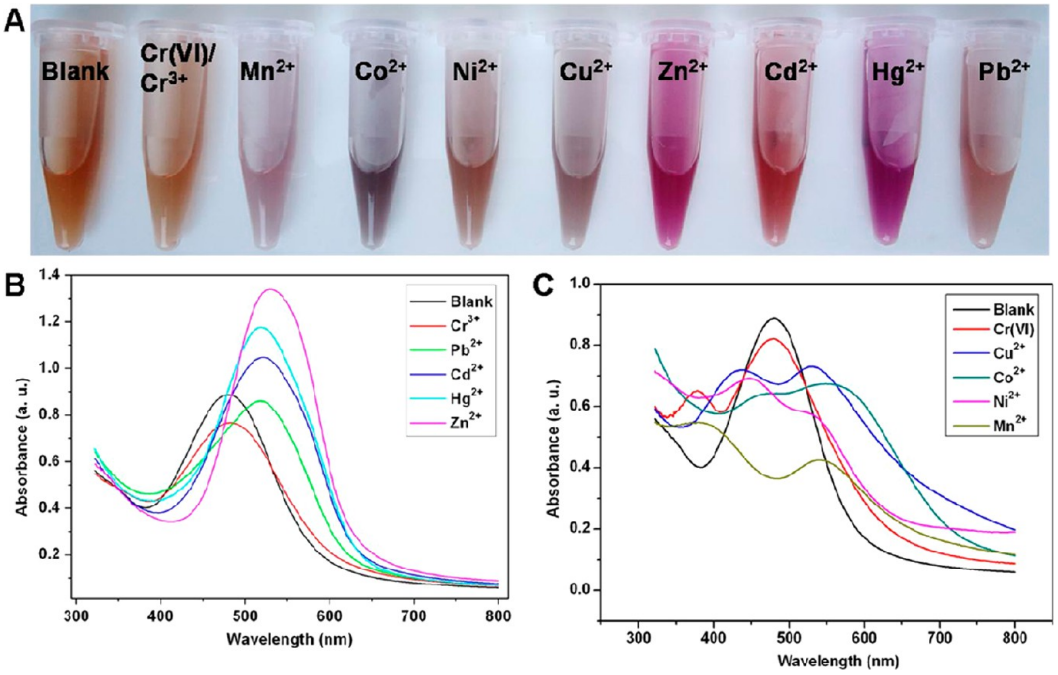

Figure 7. Colorimetric response of the developed reagent to 10 types of heavy metal ions. (A) Digital photos of the developed reagent after exposure to 20 μM of different kinds of heavy metal ions. (B and C) Corresponding UV−vis absorption spectra of the developed reagent in the presence of heavy metal ions.

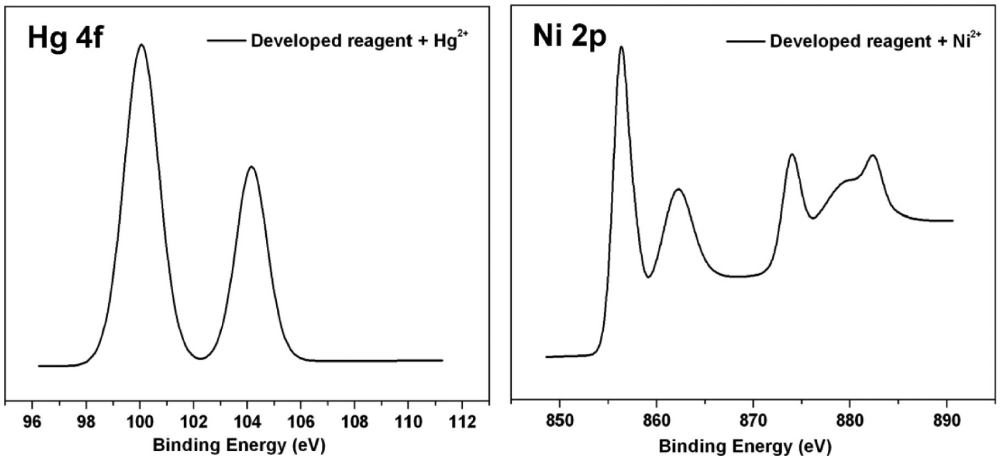

Figure 8. The Hg 4f and Ni 2p XPS spectra recorded on the mixtures of the developed reagent in the presence of Hg^{2+} and Ni^{2+}, respectively.

order: Zn^{2+} > Hg^{2+} > Pb^{2+} > Co^{2+} > Cu^{2+} > 1.0 > Cd^{2+} > Ni^{2+} > Mn^{2+} > Cr(VI) > Cr^{3+}. When the mixture of CTAB and dithizone products is mixed with Zn^{2+}, Hg^{2+}, Pb^{2+}, Co^{2+}, and Cu^{2+}, respectively, their chelates dominated in the solution induce the obvious color changes. The reason for the phenomenon might be that the multiple coordination bonds form between reagents (CTAB and dithizone products) and Zn^{2+}, Hg^{2+}, Pb^{2+}, Co^{2+}, and Cu^{2+}, respectively, and d−d transitions make the obvious color changes, as shown in Figure S6, panel C, of the Supporting Information. Besides, cation−π interactions between these heavy metal ions and the dithizone products of $C_6H_5O^-$ should happen.[51] Moreover, the colorimetric and SPR responses of the mixture of CTAB and dithizone products to heavy metal ions are improved by the presence of AuNPs and distinct for a particular metal ion (see Figure 7). The reason for the phenomenon might be due to the d−d transitions between AuNPs and heavy metal ions and the aggregation of AuNPs induced by heavy metal ions.

The interactions between the developed reagent and heavy metal ions were investigated from analysis of the experimental FT-IR and XPS spectra. The FT-IR spectra of the developed reagent in the presence of two types of representative heavy metal ions (i.e., Hg^{2+} and Ni^{2+}) are shown in Figure 5. After addition of Hg^{2+} to the developed reagent, the new vibration peak appears at 466 cm^{-1}, which can be unambiguously assigned to the Hg−N stretching vibration [ν(Hg−N)] (see Figure 5A).[52,53] At the same time, the N···H stretch at 3538 cm^{-1} disappears (see Figure 5B), as is the case for addition of Ni^{2+}. Furthermore, the interactions between the developed reagent and targets of heavy metal ions can be inspected by XPS characterizations. The spectra of the Hg 4f and Ni 2p components show the core peaks at 100.1 and 856.3 eV, which can be assigned to the binding energies of Hg−N and Ni−N,

dx.doi.org/10.1021/la400909b | Langmuir 2013, 29, 7591−7599

respectively (see Figure 8).[54,55] The experimental FT-IR and XPS results confirm that the M^{n+}−N bonds are formed between $[SCH_2N_4]^{2-}$ and heavy metal ions, which is the reason for M^{n+}-induced aggregation of the modified AuNPs (see Figure S2 of the Supporting Information).

In order to assess the validity of the developed reagent, the method was applied to colorimetric analysis of 10 types of heavy metal ions in tap water. The spiked samples of 80 μM heavy metal ions in tap water were mixed with the developed reagent at a volume ratio of 1:3. The final concentrations of the tested heavy metal ions are 20 μM. The corresponding color and UV−vis absorption spectra changes of the developed reagent in the presence of heavy metal ions in tap water are in good agreement with that performed in Milli-Q water (see Figure S8 of the Supporting Information).

Colorimetric response of the developed reagent to the mixtures of two or more kinds of heavy metal ions and sensitivity optimization are under study.

CONCLUSIONS

In summary, we have developed a novel reagent for colorimetric response to 10 types of heavy metal ions, including Cr(VI), Cr^{3+}, Mn^{2+}, Co^{2+}, Ni^{2+}, Cu^{2+}, Zn^{2+}, Cd^{2+}, Hg^{2+}, and Pb^{2+}. The distinct color change for Mn^{2+}, Co^{2+}, Ni^{2+}, Cu^{2+}, Zn^{2+}, Cd^{2+}, Hg^{2+}, and Pb^{2+} is instantaneous. The color change results from the multiple effects, such as electronic transitions, cation−π interactions, formation of coordination bonds, and aggregation of AuNPs induced by heavy metal ions. The different combining capacities of heavy metal ions to the modifiers results in different aggregation of the modified AuNPs. The charge transfer from $[SCH_2N_4]^{2-}$ to Cr(VI)/Cu^{2+}/Co^{2+}/Ni^{2+}/Mn^{2+} might cause the different excited states to be mixed in these heavy metal ions, resulting in the new UV−vis absorption peaks in the region of 360−460 nm. The experimental and simulated results prove that dithizone reacts with NaOH to produce $C_6H_5O^-$ and $[SCH_2N_4]^{2-}$. The FT-IR and XPS data imply interactions between CTAB headgroups $[-(CH_3)_3NBr]$ and AuNPs, inducing CTAB molecules to absorb on AuNPs and confirm that AuNPs are modified by $[SCH_2N_4]^{2-}$ through Au−S bonds and the M^{n+}−N bonds are formed between heavy metal ions and $[SCH_2N_4]^{2-}$. Cation−π interactions between heavy metal ions and $C_6H_5O^-$ should happen in solution. In addition, the analysis results of heavy metal ions in tap water using the developed reagent are in good agreement with that performed in Milli-Q water.

ASSOCIATED CONTENT

Supporting Information

Digital photos (Figures S1, S3, S5, S6, and S8), TEM images of the modified AuNPs aggregation induced by heavy metal ions [i.e., Hg^{2+} and Co^{2+} (Figure S2)], UV−vis absorption spectra (Figures S1, S4, S7, and S8), and Table S1. This material is available free of charge via the Internet at http://pubs.acs.org.

AUTHOR INFORMATION

Corresponding Author

*A.W.: e-mail, aiguo@nimte.ac.cn. L.C.: e-mail, chenliang@nimte.ac.cn.

Notes

The authors declare no competing financial interest.

ACKNOWLEDGMENTS

This work was supported by the National High-Tech Program (863, Grant SS2012AA063202), the program of the Zhejiang Provincial Natural Science Foundation of China under Grant R5110230, Natural Science Foundation of China under Grant 31128007, the Hundred Talents Program of Chinese Academy of Sciences, and the program of Bureau of Academy-Locality Cooperation Chinese Academy of Sciences, Ningbo Science and Technology Bureau (Grants 2011C50009, 2009B21005 and 2011A610121), and the projects sponsored by the Scientific Research Foundation for the Returned Overseas Chinese Scholars, and the States of Ministry of Education & Ministry of Human Resources & Social Security. Y.L. also thanks Dr. Yujie Zhang, Zhuqing Wang, Lijing Miao, Tianhua Li, Ningning Yang, Dr. Tianxiang Chen, Dr. Leyong Zeng, Dr. Xinmei Zhao, and Yuexia Gao for helpful discussions.

REFERENCES

(1) Kim, Y.; Johnson, R. C.; Hupp, J. T. Gold Nanoparticle-Based Sensing of "Spectroscopically Silent" Heavy Metal Ions. *Nano Lett.* **2001**, *1*, 165−167.

(2) Zhang, Y.; Leng, Y.; Miao, L.; Xin, J.; Wu, A. The Colorimetric Detection of Pb^{2+} by Using Sodium Thiosulfate and Hexadecyl Trimethyl Ammonium Bromide Modified Gold Nanoparticles. *Dalton Trans.* **2013**, *42*, 5485−5490.

(3) Slocik, J. M.; Zabinski, J. S., Jr.; Phillips, D. M.; Naik, R. R. Colorimetric Response of Peptide-Functionalized Gold Nanoparticles to Metal Ions. *Small* **2008**, *4*, 548−551.

(4) Bootharaju, M. S.; Pradeep, T. Investigation into the Reactivity of Unsupported and Supported Ag_7 and Ag_8 Clusters with Toxic Metal Ions. *Langmuir* **2011**, *27*, 8134−8143.

(5) Xia, F.; Zuo, X.; Yang, R.; Xiao, Y.; Kang, D.; Vallée-Bélisle, A.; Gong, X.; Yuen, J. D.; Hsu, B. B. Y.; Heeger, A. J.; Plaxco, K. W. Colorimetric Detection of DNA, Small Molecules, Proteins, and Ions Using Unmodified Gold Nanoparticles and Conjugated Polyelectrolytes. *Proc. Natl. Acad. Sci. U.S.A* **2010**, *107*, 10837−10841.

(6) Lou, T.; Chen, L.; Chen, Z.; Wang, Y.; Chen, L.; Li, J. Colorimetric Detection of Trace Copper Ions Based on Catalytic Leaching of Silver-Coated Gold Nanoparticles. *ACS Appl. Mater. Interfaces* **2011**, *3*, 4215−4220.

(7) Li, J.; Chen, L.; Lou, T.; Wang, Y. Highly Sensitive SERS Detection of As^{3+} Ions in Aqueous Media using Glutathione Functionalized Silver Nanoparticles. *ACS Appl. Mater. Interfaces* **2011**, *3*, 3936−3941.

(8) Kong, B.; Zhu, A.; Luo, Y.; Tian, Y.; Yu, Y.; Shi, G. Sensitive and Selective Colorimetric Visualization of Cerebral Dopamine Based on Double Molecular Recognition. *Angew. Chem., Int. Ed.* **2011**, *50*, 1837−1840.

(9) Lou, T.; Chen, Z.; Wang, Y.; Chen, L. Blue-to-Red Colorimetric Sensing Strategy for Hg^{2+} and Ag^{+} via Redox-Regulated Surface Chemistry of Gold Nanoparticles. *ACS Appl. Mater. Interfaces* **2011**, *3*, 1568−1573.

(10) Miao, L.; Xin, J.; Shen, Z.; Zhang, Y.; Wang, H.; Wu, A. Exploring a New Rapid Colorimetric Detection Method of Cu^{2+} with High Sensitivity and Selectivity. *Sens. Actuators, B* **2013**, *176*, 906−912.

(11) Du, P.; Li, H.; Mei, Z.; Liu, S. Electrochemical DNA Biosensor for the Detection of DNA Hybridization with the Amplification of Au Nanoparticles and CdS Nanoparticles. *Bioelectrochemistry* **2009**, *75*, 37−43.

(12) Zhang, F.; Zeng, L.; Zhang, Y.; Wang, H.; Wu, A. A Colorimetric Assay Method for Co^{2+} Based on Thioglycolic Acid Functionalized Hexadecyl Trimethyl Ammonium Bromide Modified Au Nanoparticles (NPs). *Nanoscale* **2011**, *3*, 2150−2154.

(13) Leng, Y.; Zhang, F.; Zhang, Y.; Fu, X.; Weng, Y.; Chen, L.; Wu, A. A Rapid and Sensitive Colorimetric Assay Method for Co^{2+} Based on the Modified Au Nanoparticles (NPs): Understanding the Involved

Interactions from Experiments and Simulations. *Talanta* **2012**, *94*, 271−277.
(14) Yuan, C.; Zhang, K.; Zhang, Z.; Wang, S. Highly Selective and Sensitive Detection of Mercuric Ion Based on a Visual Fluorescence Method. *Anal. Chem.* **2012**, *84*, 9792−9801.
(15) Zhu, H.; Zhang, W.; Zhang, K.; Wang, S. Dual-emission of a Fluorescent Graphene Oxide−Quantum Dot Nanohybrid for Sensitive and Selective Visual Sensor Applications Based on Ratiometric Fluorescence. *Nanotechnology* **2012**, *23*, 315502 (8pp).
(16) Fries, K. H.; Driskell, J. D.; Sheppard, G. R.; Locklin, J. Fabrication of Spiropyran-Containing Thin Film Sensors Used for the Simultaneous Identification of Multiple Metal Ions. *Langmuir* **2011**, *27*, 12253−12260.
(17) Fu, X.; Lou, T.; Chen, Z.; Lin, M.; Feng, W.; Chen, L. "Turn-on" Fluorescence Detection of Lead Ions Based on Accelerated Leaching of Gold Nanoparticles on the Surface of Graphene. *ACS Appl. Mater. Interfaces* **2012**, *4*, 1080−1086.
(18) Stoica, A.; Peltea, M.; Baiulescu, G.; Ionica, M. Determination of Cobalt in Pharmaceutical Products. *J. Pharm. Biomed. Anal.* **2004**, *36*, 653−656.
(19) Yuzefovsky, A. I.; Lonardo, R. F.; Wang, M.; Michel, R. G. Determination of Ultra-trace Amounts of Cobalt in Ocean Water by Laser-excited Atomic Fluorescence Spectrometry in a Graphite Electrothermal Atomizer with Semi on-line Flow Injection Preconcentration. *J. Anal. At. Spectrom.* **1994**, *9*, 1195−1202.
(20) Turnlund, J. R. Human Whole-body Copper Metabolism. *Am. J. Clin. Nutr.* **1998**, *67*, 960−964.
(21) Dunnick, J. K.; Elwell, M. R.; Radovsky, A. E.; Benson, J. M.; Hahn, F. F.; Nikula, K. J.; Barr, E. B.; Hobbs, C. H. Comparative Carcinogenic Effects of Nickel Subsulfide, Nickel Oxide, or Nickel Sulfate Hexahydrate Chronic Exposures in the Lung. *Cancer Res.* **1995**, *55*, 5251−5256.
(22) Serafin, T.; Verity, A. Oxidative Mechanisms Underlying Methyl Mercury Neurotoxicity. *Int. J. Dev. Neurosci.* **1991**, *9*, 147−153.
(23) Nader, R.; George, C.; Muriel, W.; Lawrence, C.; Christine, F.; John, S.; Louis, D. Incidence of Lead Poisoning in Young Children from Inner-City, Suburban, and Rural Communities. *Ther. Drug Monit.* **1993**, *15*, 71−74.
(24) Knecht, M. R.; Sethi, M. Bio-inspired Colorimetric Detection of Hg^{2+} and Pb^{2+} Heavy Metal Ions using Au Nanoparticles. *Anal. Bioanal. Chem.* **2009**, *394*, 33−46.
(25) Hung, Y.; Hsiung, T.; Chen, Y.; Huang, Y.; Huang, C. Colorimetric Detection of Heavy Metal Ions Using Label-Free Gold Nanoparticles and Alkanethiols. *J. Phys. Chem. C* **2010**, *114*, 16329−16334.
(26) Lee, Y.; Nan, F.; Chen, M.; Wu, H.; Ho, C.; Chen, Y.; Huang, C. Detection and Removal of Mercury and Lead Ions by Using Gold Nanoparticle-based Gel Membrane. *Anal. Methods* **2012**, *4*, 1709−1717.
(27) Guo, Y.; Wang, Z.; Qu, W.; Shao, H.; Jiang, X. Colorimetric Detection of Mercury, Lead and Copper Ions Simultaneously Using Protein-functionalized Gold Nanoparticles. *Biosens. Bioelectron.* **2011**, *26*, 4064−4069.
(28) Simon, A.; MacAleese, L.; Maître, P.; Lemaire, J.; McMahon, T. B. Fingerprint Vibrational Spectra of Protonated Methyl Esters of Amino Acids in the Gas Phase. *J. Am. Chem. Soc.* **2007**, *129*, 2829−2840.
(29) Leng, Y.; Zhang, M.; Song, C.; Chen, M.; Lin, Z. A Semi-empirical and Ab Initio Combined Approach for the Full Conformational Searches of Gaseous Lysine and Lysine-H_2O Complex. *J. Mol. Struct.: THEOCHEM* **2008**, *858*, 52−65.
(30) Xu, X.; Yu, W.; Huang, Z.; Lin, Z. Comprehensive Density Functional Theory Study on the Mechanism of Activation of the Nonapeptide Hormone Oxytocin by Metal Ions. *J. Phys. Chem. B* **2010**, *114*, 1417−1423.
(31) Jana, N. R.; Gearheart, L.; Murphy, C. J. Wet Chemical Synthesis of High Aspect Ratio Cylindrical Gold Nanorods. *J. Phys. Chem. B* **2001**, *105*, 4065−4067.
(32) Ermakov, A. I.; Belousov, V. V. Relaxation of STO-3G and 6-31G* Basis Set Functions in the Series of LiF Isoelectronic Molecules of Second Row Elements. *J. Struct. Chem.* **2007**, *48*, 6−15.
(33) Guillaume, M.; Ruud, K.; Rizzo, A.; Monti, S.; Lin, Z.; Xu, X. Computational Study of the One- and Two-Photon Absorption and Circular Dichroism of (L)-Tryptophan. *J. Phys. Chem. B* **2010**, *114*, 6500−6512.
(34) Merrick, J. P.; Moran, D.; Radom, L. An Evaluation of Harmonic Vibrational Frequency Scale Factors. *J. Phys. Chem. A* **2007**, *111*, 11683−11700.
(35) Tian, S. X.; Xu, K. Z.; Huang, M. B.; Chen, X. J.; Yang, J. L.; Jia, C. C. Theoretical Study on Infrared Vibrational Spectra of Boric-Acid in Gas-Phase Using Density Functional Methods. *J. Mol. Struct.: THEOCHEM* **1999**, *459*, 223−227.
(36) Kryachko, E. S.; Remacle, F. Implementation of simple logic gates on gold−ammonia bonding patterns in different charge states. *Mol. Phys.* **2008**, *106*, 521−530.
(37) Tanino, H.; Takahashi, K.; Tajima, M.; Kato, M.; Yao, T. Optical Properties and Raman Spectra of the Quasi-One-Dimensional Gold Complexes AuX_2 Dibenzylsulfide (X_2 = Cl_2, ClBr, Br_2). *Phys. Rev. B* **1988**, *38*, 8327−8335.
(38) Jana, N. R.; Gearheart, L. A.; Obare, S. O.; Johnson, C. J.; Edler, K. J.; Mann, S.; Murphy, C. J. Liquid Crystalline Assemblies of Ordered Gold Nanorods. *J. Mater. Chem.* **2002**, *12*, 2909−2912.
(39) Sau, T. K.; Murphy, C. J. Seeded High Yield Synthesis of Short Au Nanorods in Aqueous Solution. *Langmuir* **2004**, *20*, 6414−6420.
(40) Zhu, C.; Peng, H.; Zeng, J.; Liu, J.; Gu, Z.; Xia, Y. Facile Synthesis of Gold Wavy Nanowires and Investigation of Their Growth Mechanism. *J. Am. Chem. Soc.* **2012**, *134*, 20234−20237.
(41) Cheng, W.; Dong, S.; Wang, E. Synthesis and Self-Assembly of Cetyltrimethylammonium Bromide-Capped Gold Nanoparticles. *Langmuir* **2003**, *19*, 9434−9439.
(42) Wang, B.; Wang, X.; Lou, W.; Hao, J. Gold-ionic Liquid Nanofluids with Preferably Tribological Properties and Thermal Conductivity. *Nanoscale Res. Lett.* **2011**, *6*, 259.
(43) Gao, X.; Zhang, Y.; Weaver, M. J. Adsorption and Electro-oxidative Pathways for Sulfide on Gold as Probed by Real-time Surface-enhanced Raman Spectroscopy. *Langmuir* **1992**, *8*, 668−672.
(44) Sanov, A.; Droz-Georget, T.; Zyrianov, M.; Reisler, H. Photofragment Imaging of HNCO Decomposition: Angular Anisotropy and Correlated Distributions. *J. Chem. Phys.* **1997**, *106*, 7013−7022.
(45) Johnson, R. S.; Schachman, H. K. Communication Between Catalytic and Regulatory Subunits in Ni(II)- and Co(II)-Aspartate Transcarbamoylase. Ligand-Promoted Structural Alterations at the Intersubunit Bonding Domains. *J. Biol. Chem.* **1983**, *258*, 3528−3538.
(46) Mastropaolo, D.; Thich, J. A.; Potenza, J. A.; Schugar, H. J. Molecular Structure and Electronic Spectra of Bis [β-Mercapto-β',β''-Dimethylethylamino]Cobaltate(II), $Co[SC(CH_3)_2CH_2NH_2]_2$. *J. Am. Chem. Soc.* **1977**, *99*, 424−429.
(47) McMillin, D. R.; Holwerda, R. A.; Gray, H. B. Preparation and Spectroscopic Studies of Cobalt(II)-Stellacyanin. *Proc. Natl. Acad. Sci. U.S.A.* **1974**, *71*, 1339−1341.
(48) Vašák, M. Spectroscopic Studies on Cobalt(II) Metallothionein: Evidence for Pseudotetrahedral Metal Coordination. *J. Am. Chem. Soc.* **1980**, *102*, 3953−3955.
(49) *Quality Standard for Ground Water of the National Standards of the People's Republic of China*, GB/T 14848-93, Department of Water Resources Management: China, 1993.
(50) Moore, E. A.; Janes, R. *Metal−Ligand Bonding*; The Open University: Milton Keynes, U.K., 2004.
(51) Mahadevi, A. S.; Sastry, G. N. Cation−π Interaction: Its Role and Relevance in Chemistry, Biology, and Material Science. *Chem. Rev.* **2013**, *113*, 2100−2138.
(52) Alex, S.; Savoie, R.; Corbeil, M.; Beauchamp, A. Complexation of Glycylglycine by the Methylmercury Cation: A Vibrational Spectroscopy and X-ray Diffraction Study. *Can. J. Chem.* **1986**, *64*, 148−157.

(53) Bharara, M. S.; Parkin, S.; Atwood, D. A. Mercury(II) 2-Aminoethanethiolate Clusters: Intramolecular Transformations and Mechanisms. *Inorg. Chem.* **2006**, *45*, 7261−7268.
(54) Wyckoff, R. Crystal Structures, 2nd ed.; Wiley Interscience Publishers, Inc.: New York, 1963.
(55) LaSurface com, http://www.lasurface.com (accessed May 18, 2012).